CHAPTER 6

Transport of Solutes into Emulsion Liquid Membranes: Modeling and Simulation

CHAPTER 6

TRANSPORT OF SOLUTES INTO EMULSION LIQUID MEMBRANES: MODELING AND SIMULATION

In order to get a deeper understanding of the solute transport in liquid membranes many mathematical models have been proposed. Cahn and Li (1974) were the first to model the solute transport in emulsion liquid membranes. They analyzed experiments involving phenol removal from wastewater by assuming that the emulsion globules are internally well mixed and the rate of phenol transfer is directly proportional to the difference between the solute concentrations in the solution and the emulsion globule. However, they found that the effective permeability varies with time. Boyadzhiev *et al.* (1978) followed this same analysis. Kremesec (1981) and Kremesec and Slattery (1982) used planar geometry and summed mass transfer resistances through the continuous, membrane and internal phases. In their method geometric and internal circulation effects are lumped up into the overall mass transfer coefficient.

Ho and Li (1992) present a comprehensive review of the various models developed to describe transport of solutes through ELMs. The models may be classified in two categories: the spherical shell approach and the emulsion globule approach. The spherical shell approach assumes that the mass transfer resistance is diffusion in the spherical 'shell' of the membrane phase of constant thickness between the external and the internal phases. All the above-mentioned investigators used his concept to develop their models.

There are numerous shortcomings associated with the spherical shell models for the extraction of solute in ELMs. These models do not take the diffusion of solute in emulsion globules into account. This can result in variation of mass transfer coefficient with time. Moreover they do not account for the effect of the rate at which the internal reagent is consumed. Kopp *et al.* (1978) recognized this problem, and proposed that the diffusion process be described in terms of a boundary at which the reaction occurs and which moves in towards the globule center as the internal reagent is consumed. However, their use of the solution for the equivalent planar problem to represent the transport in a spherical geometry limits the application of their work limits the range of applicability of their work. To overcome these short comings Ho *et al.*(1982) developed a model based on first principles that is known as the 'Advancing Front Model'.

The advancing front model is regarded as the standard model for simulating the transport of phenol and other solutes into the internal phase of the emulsion liquid membranes. It assumes that the reaction inside the globule is irreversible and instantaneous. Bunge and Noble (1984) developed the reversible reaction model in which the reaction between the solute and the internal reagent is a reversible one. Over the years minor modifications to both these models have appeared in order to incorporate the effect of leakage (Borwankar *et al.*1988), external phase mass transfer coefficient (Stroeve and Varanasi 1984) etc. However till date the extraction performance using ELMs as predicted by these models have not been tested against experimental data obtained under varied extraction conditions. Hence it was decided to test the efficacy of both these models with the data on extraction of phenols.

6.1 THE ADVANCING FRONT MODEL

The basic concept of the advancing front model is that the ELMs when dispersed in the continuous phase forms a monodisperse non-coalescing collection of spherical droplets. The solute taken up from the continuous phase diffuses through the globule to a reaction front, where it is removed by an instantaneous and irreversible chemical reaction. The

reaction front advances in towards the globule center as the internal reagent is consumed as shown in Fig. 6.1.

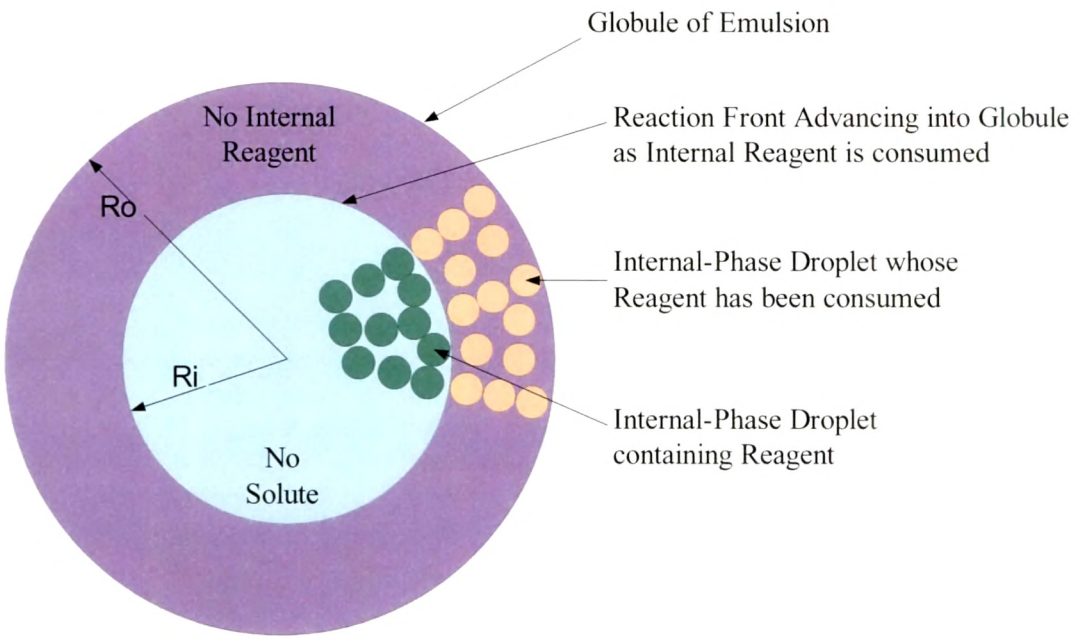

Fig. 6.1:Schematic diagram of the advancing front model

The advancing front model assumes the following :

i. The membrane and the external phases are completely immiscible , and the membrane and internal phases are also completely immiscible.
ii. All emulsion globules and internal phase droplets are spherical, and the size of both globules and droplets are represented by a single Sauter men diameter for globules and a single Sauter mean diameter for droplets.
iii. There is no internal circulation within the globules.
iv. There is no coalescence and redispersion of the emulsion globules
v. The solute from the external phase diffuses into the globule to a reaction front where it is removed by reaction with the internal reagent. The reaction is assumed to be instantaneous and irreversible. The reaction front separates the inner region containing no solute from the outer region in which the internal phase has been consumed and contains no reagent as shown in Fig. 6.1. The reaction front moves towards the globule center as the internal reagent is consumed
vi. Local phase equilibrium holds between the membrane and internal droplet phase. The solute concentration within the globules can be described in terms of the average local concentration.
vii. The system is well agitated so external phase mass transfer resistance can be neglected

viii. Membrane leakage is neglected.
ix. At the globule surface the solute concentration in the membrane phase is in equilibrium with that in the external phase.

Mathematical description

The equations describing the concentrations of the solute in the globules and in the external continuous phase are (Ho *et al.* 1982)

Globules

$$\frac{\partial C}{\partial t} = \left(\frac{D_{eff}}{r^2}\right) \frac{\partial}{\partial r}\left(r^2 \frac{\partial C}{\partial r}\right) \qquad R_f(t) \le r \le R \qquad 6.1$$

$$t = 0 \qquad C = 0 \qquad (r < R) \qquad 6.2$$

$$r = R \qquad C = \alpha C_e \qquad (t > 0) \qquad 6.3$$

$$r = R_f(t) \qquad C = 0 \qquad (t > 0) \qquad 6.4$$

External phase

$$-V_e \frac{dC_e}{dt} = n(4\pi R^2) D_{eff} \left(\frac{\partial C}{\partial r}\right)_{r=R} \qquad 6.5$$

$$= \frac{3}{R}(V_m + V_i) D_{eff} \left(\frac{\partial C}{\partial r}\right)_{r=R} \qquad 6.6$$

$$t = 0 \qquad C_e = C_{eo} \qquad 6.7$$

The material balance over the reaction front gives

$$-\frac{V_i}{V_m + V_i} C_{io} \left(\frac{dR}{dt}\right) = D_{eff} \left(\frac{\partial c}{\partial r}\right)_{r = Rf(t)} \qquad 6.8$$

$$t = 0 \qquad R_f = R \qquad 6.9$$

R_f denotes the position of the advancing front.

These equations are inherently non linear and cannot be solved analytically. Ho *et al* . (1982) rendered Eqs. (6.1) to (6.9) dimensionless form by defining :

$\eta = r / R$ $\chi = R_f / R$ $\tau = \varepsilon D_{eff} t / R^2$ $g = C / \alpha C_{eo}$

$h = C_e / C_{eo}$ $\varepsilon = \dfrac{\alpha C_{eo}}{(V_i / V_m + V_i) C_{io}}$ 6.10

$E = 3(\dfrac{C_{io} V_i}{C_{eo} V_e})$

The resulting dimensionless model equations were solved by Ho *et al.* (1982) using perturbation techniques. The zero order perturbation solutions are

$$\phi_0 = \frac{E}{3}(\chi^3 - B^3)(1-\delta) \qquad 6.11$$

$$h_0 = \frac{E}{3}(\chi^3 - B^3) \qquad 6.12$$

$$\tau_0 = \frac{1}{E}[(1+\frac{1}{2B})\ln(\frac{\chi^3 - B^3}{1-B^3}) - \frac{3}{2B}\ln(\frac{\chi - B}{1-B})] - \frac{\sqrt{3}}{EB}[\tan^{-1}(\frac{2\chi + B}{\sqrt{3}B}) - \tan^{-1}(\frac{2+B}{\sqrt{3}B})] \qquad 6.13$$

where $$B = (1+\frac{3}{E})^{1/3} \qquad 6.14$$

the subscript $_0$ indicates zero order solution

Two parameters –the equilibrium distribution coefficient for the solute between the reacted emulsion mixture and the external feed phase (α) and the effective diffusivity of the solute in emulsion mixture- are necessary for the prediction of extraction of solute using the advancing front model.

Equilibrium distribution coefficient

The average concentration of the diffusing solute in the exhausted region of the emulsion ($r > R_f$) is

$$C = (\frac{V_i C_i + V_m C_m}{V_i + V_m}) = (\frac{V_i / \alpha^I + V_m}{V_i + V_m}) C_m \qquad 6.15$$

where C_m and C_i are the solute concentration in the membrane phase and the reacted internal phase and α^I is the distribution coefficient of solute between the membrane phase and the depleted internal phases at equilibrium. Because the initial concentration of the

internal reagent is relatively low the model assumes α^I = K, the distribution coefficient obtained for the oil/external phase.

At the globule surface, we have equilibrium between the external aqueous phase and the membrane phase. Thus

$$C_m = \alpha^I C_e \qquad \text{at r = R.} \qquad 6.16$$

Further the model also assumes equilibrium between the external phase and the emulsion at the globule surface. Hence,

$$C = \alpha C_e \qquad \text{at r = R} \qquad 6.17$$

combining Eqs. 6.15 to 6.17 one gets

$$\alpha = \left(\frac{V_i + \alpha^I V_m}{V_i + V_m}\right) \qquad 6.18$$

Effective Diffusivity

The effective diffusivity $D^I eff$ of the solute in the emulsion mixture, based on a concentration driving force defined in terms of the membrane phase concentration C_m, can be estimated from the Jefferson-Witzell -Sibbett equation (Jefferson *et al.*1956, Crank 1975 and Ho *et al.*1982) given below which was originally developed to estimate the thermal conductivity of dispersions.

$$D^I_{eff} = D_m\left(\frac{4(1+2p)^2 - \pi}{4(1+2p)^2}\right) + \frac{\pi}{4(1+2p)^2}\left(\frac{(1+2p)D_A D_m}{D_m + 2pD_A}\right) \qquad 6.19$$

where

$$D_A = \frac{2(D_i/\alpha^I)D_m}{(D_i/\alpha^I) - D_m}\left[\frac{D_i/\alpha^I}{(D_i/\alpha^I) - D_m}\ln\frac{(D_i/\alpha^I)}{D_m} - 1\right] \qquad 6.20$$

$$p = 0.403\left(\frac{V_i}{V_m + V_i}\right)^{-1/3} - 0.5 \qquad 6.21$$

D_i is the solute diffusivity in the reacted internal phase and D_m is the solute diffusivity in the membrane phase. The effective diffusivity based on the average concentration C in the emulsion mixture can be related to D^I_{eff} through the equation

$$D_{eff}\frac{dC}{dr} = D^{I}_{eff}\frac{dC_m}{dr} \qquad 6.22$$

combining Eqs. 6.15, 6.18 and 6.22 we obtain

$$D_{eff} = (\frac{\alpha^{I}}{\alpha})D^{I}_{eff} \qquad 6.23$$

6.1.1 Prediction of extraction profile using the advancing front model

The zero order perturbation solutions by Ho *et al.* (Eq. 6.11 to Eq.6.14) could be conveniently utilized to predict τ_0 (dimensionless time) required for achieving a specified separation h_0. The calculation procedure adopted is simple, a value of h_0 is selected, and then the value of E and B are calculated with the help of Eq.(6.10) and Eq.(6.14) respectively. Knowing the value of h_0, E and B, the value of χ is calculated with the help of Eq. (6.12). Next the value of τ_0 (dimensionless time) is calculated using Eq.(6.13) by substituting the respective values of E, B and χ. Once τ is known, the time 't' can be evaluated by the substitution of appropriately calculated values of parameter D_{eff}, R and ε in the following equation:

$\tau = \varepsilon D_{eff} t / R^2$

For a sample calculation, we can consider the extraction of p-cresol using ELMs (Run no. 140, TableD.1) with kerosene as external phase, NaOH solution as internal phase with ϕ = 0.45, C_{io} = 0.3 M NaOH, W_{surf} = 3% (wt), the operating parameters included TR = 1:15, the value of V_e = 0.6E-03 m^3, V_i = 18.18E-06 m^3 and V_m = 21.72E-06 m^3, N =155 rpm and C_{eo}= 4.72E-03 kmol/m^3. For this specific run at 5 minutes duration the value of C_e/C_{eo} was 0.1956, the Sauter mean diameter d_{32} = 1.1283E-03 m, distribution coefficient between kerosene and water K = 0.8189. The diffusivity of p-cresol in kerosene calculated using the Wilke-Chang correlation turns out to be D_m= 1.046E-09 m^2/s, similarly the diffusion coefficient in the internal phase turns out to be D_i = 9.26E-10 m^2/s.

Assuming K = α^{I} and substituting the calculated values of D_i and D_m in Eq.(6.19) the value of D^{I}_{eff} turns out to be 1.0837E-09 m^2/s. Using appropriate values of V_i, V_m and α^{I} in Eq.

6.18 the value of α turns out to be 0.9021. Knowing the value of α, α^I and D^I_{eff} the value of D_{eff} is next computed by Eq. (6.23) which turns out to be 9.8469E-10 m^2/s.

In order to solve the equations (6.12) and (6.13) first the values of ε and E are calculated from the relevant data using the identities in Eq.(6.10). The values of ε and E turn out to be 0.0315 and 5.78 respectively, using this value of E in Eq.(6.14) we get the value of B as 0.7836. Substituting the evaluated values E and B and the experimentally measured value of h_0 ($h_0 = C_e/C_{eo}$ = 0.1956, corresponding to a sampling time of 5 minutes) in the Eq.(6.12) the value of χ is conveniently calculated to be 0.8352. Substituting the calculated values of χ, E and B in Eq. (6.13) we get the value of τ_0 that turns out to be 3.19E-02 for this particular case. Finally using the value of D_{eff} that was evaluated to be 9.8469E-10 m^2/s, ε = 0.0315, R (radii of globule) = 5.64E-04 m along with the value of τ_0 = 3.19E-02 we get 't'= 327.14 s or 5 minutes and 27 s. Thus it is observed that for this particular case the model predicts that C_e/C_{eo} of 0.1956 (80 % extraction) to occur in 327s against the experimentally observed time of 300s, which is certainly a good prediction. Similar set of calculations made at different sampling times yield the predicted extraction profile.

This exercise was carried out for almost all runs, preferably using experimentally determined values of d_{32} and K. Selected results are presented in Figs. 6.2 to 6.5, the data points in these figures represent the actual experimental data while the predicted extraction profile using the advancing front model is shown as curves of C_e/C_{eo} versus t.

The Fig.6.2 compares the experimental versus predicted results for the case of extraction of o-cresol. It is interesting to note that as the initial concentration of o-cresol increases in the bulk solution the predicted results come closer to the experimental values Up to feed concentrations of 600 mg/dm^3 the predicted values are more than the experimental values but at 800 mg/dm^3 the predicted values are less than the experimental values. This feature is perhaps due to the basic assumption that local solute concentration does not affect the amount of reagent to react and even low solute concentrations can force reagent at reaction front to react completely.

Further it is noticed for all cases the initial rates predicted by the advancing front model is more than observed in the experimental results. This aspect could be attributed to the polydispersity of the emulsion globules, it is observed that when N = 185 rpm the experimental and predicted rates match the closest and under these conditions the homogeneity of the dispersion was more as can be seen from Fig. 4.11. When $\phi = 0.69$ the experimental and predicted results differ widely this is perhaps due to the fact that the high viscosity of the emulsions effects the dispersion behavior which could not be accounted by the advancing front model.

Fig. 6.3 compares the experimental and predicted results for 2-chlorophenol, in this case too it is seen that with increase in the 2-chlorophenol concentration the quality of fit improves. There is very good fit between the experimental and predicted values for the case of C_{eo}= 500 mg/dm^3 when C_{io} = 0.3 m also when C_{io} = 0.5 M. Fig. 6.4 shows the comparison between experimental and predicted values for p-cresol extraction. It is seen that the fit is quite good for case of C_{eo} = 500 mg/dm^3, it is found that the with increase in the C_{eo} concentration the predicted extraction profiles tend to more closely reflect the actual experimental behavior of the curves.

It was surprising to find that the matching between the experimental and predicted values for p-cresol extraction was rather poor when Treat ratio was maintained at 1:6, the predicted values were far less than the experimentally observed values. This behavior is perhaps contributed by the polydisperse nature of the emulsion globules as seen in Fig. 4.17. The Sauter mean diameter (d_{32} = 1.295 mm) obtained in this case is on the higher side, almost 70 % of droplets are of size less than d_{32} contributing to larger mass transfer area that perhaps contributes to greater extraction.

Fig. 6.5 compares the experimental and predicted results for phenol extraction. On the whole the fit between the experimental and predicted values for phenol extraction was quite poor. For all cases the predicted values were quite less than the experimental values. The possible reason for such discrepancy could stem from the model assumptions not being valid. It could also be an offshoot of the low distribution coefficient of phenol between kerosene and water.

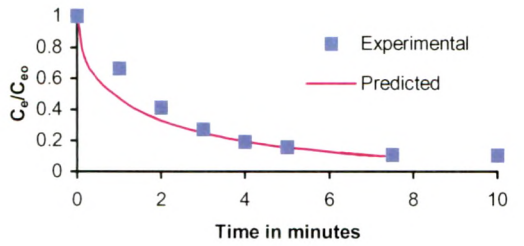

a) C_{eo} = 509 mg/dm^3

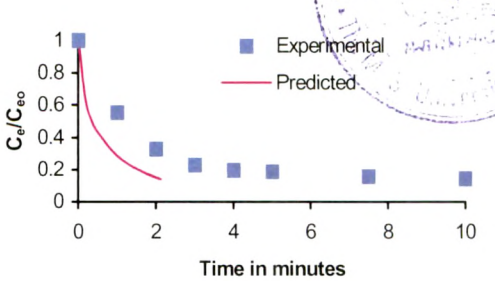

b) C_{eo} = 230 mg/dm^3

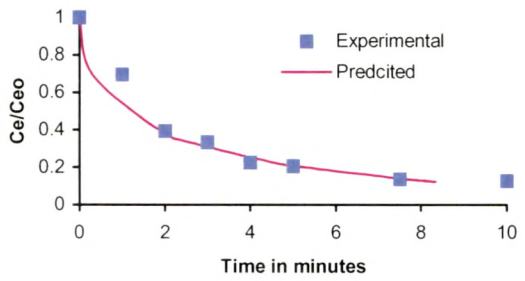

c) C_{eo} = 625 mg/dm^3

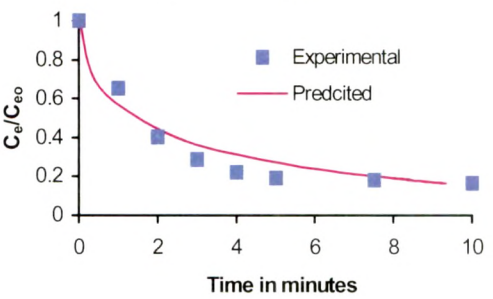

C_{eo} = 792 mg/dm^3

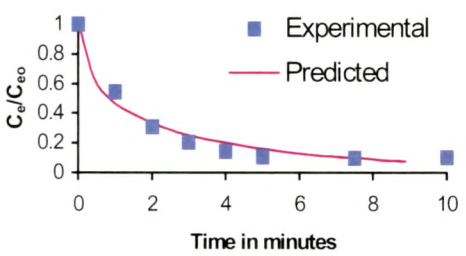

N = 185 rpm

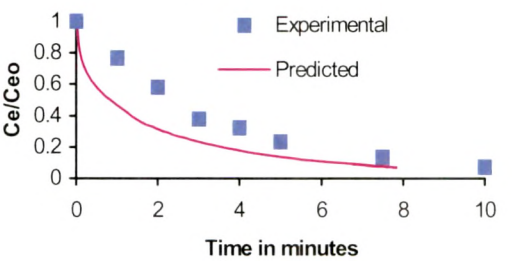

ϕ = 0.69

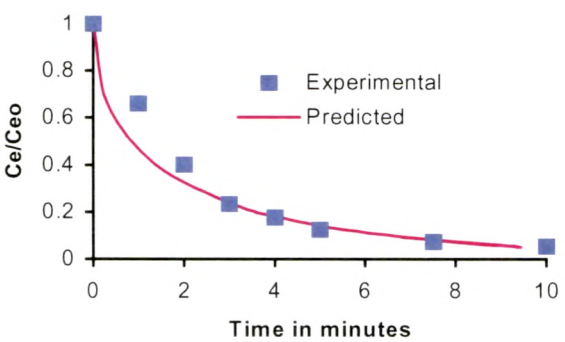

ϕ = 0.5 M

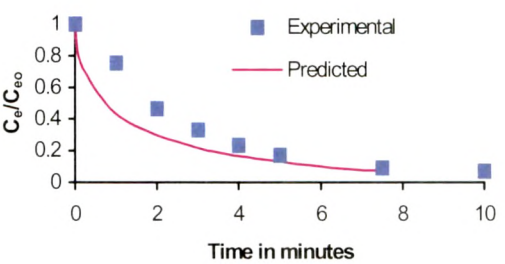

C_{io} = 0.5 M

Fig. 6.2: Comparision of experimental and predicted values using AFM (o-cresol)

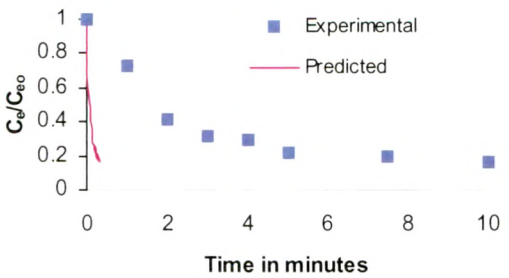

C_{eo} = 95 mg/dm^3

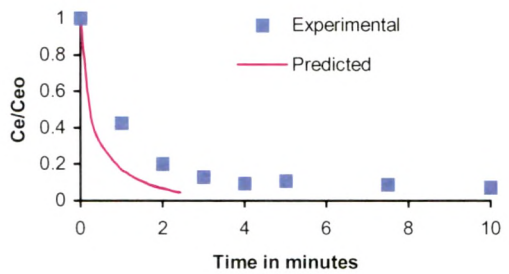

C_{eo} = 305 mg/dm^3

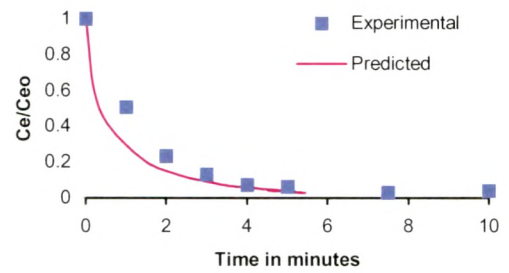

C_{eo} = 499 mg/dm^3

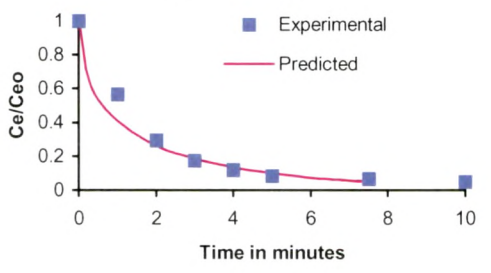

C_{io} = 0.5 M

Fig. 6.3: Comparison of experimental and predicted values using AFM (2- chlorophenol)

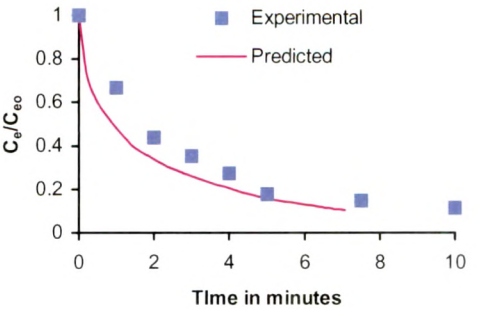

C_{eo} = 408 mg/dm^3

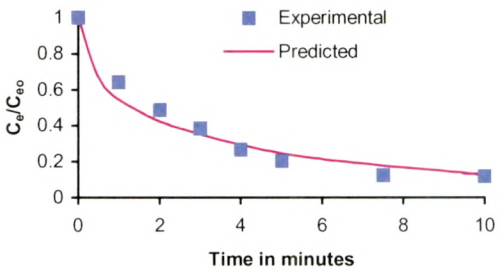

C_{eo} = 510 mg/dm^3

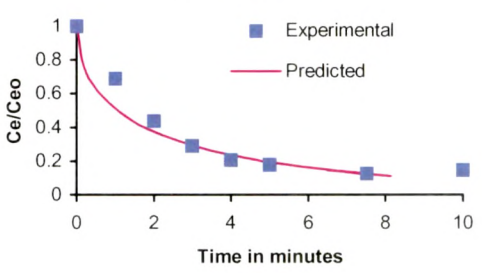

C_{eo} = 591 mg/dm^3

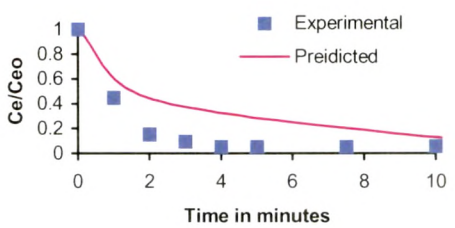

Treat ratio = 1:6

Fig. 6.4: Comparison of experimental and predicted values using AFM (p-cresol)

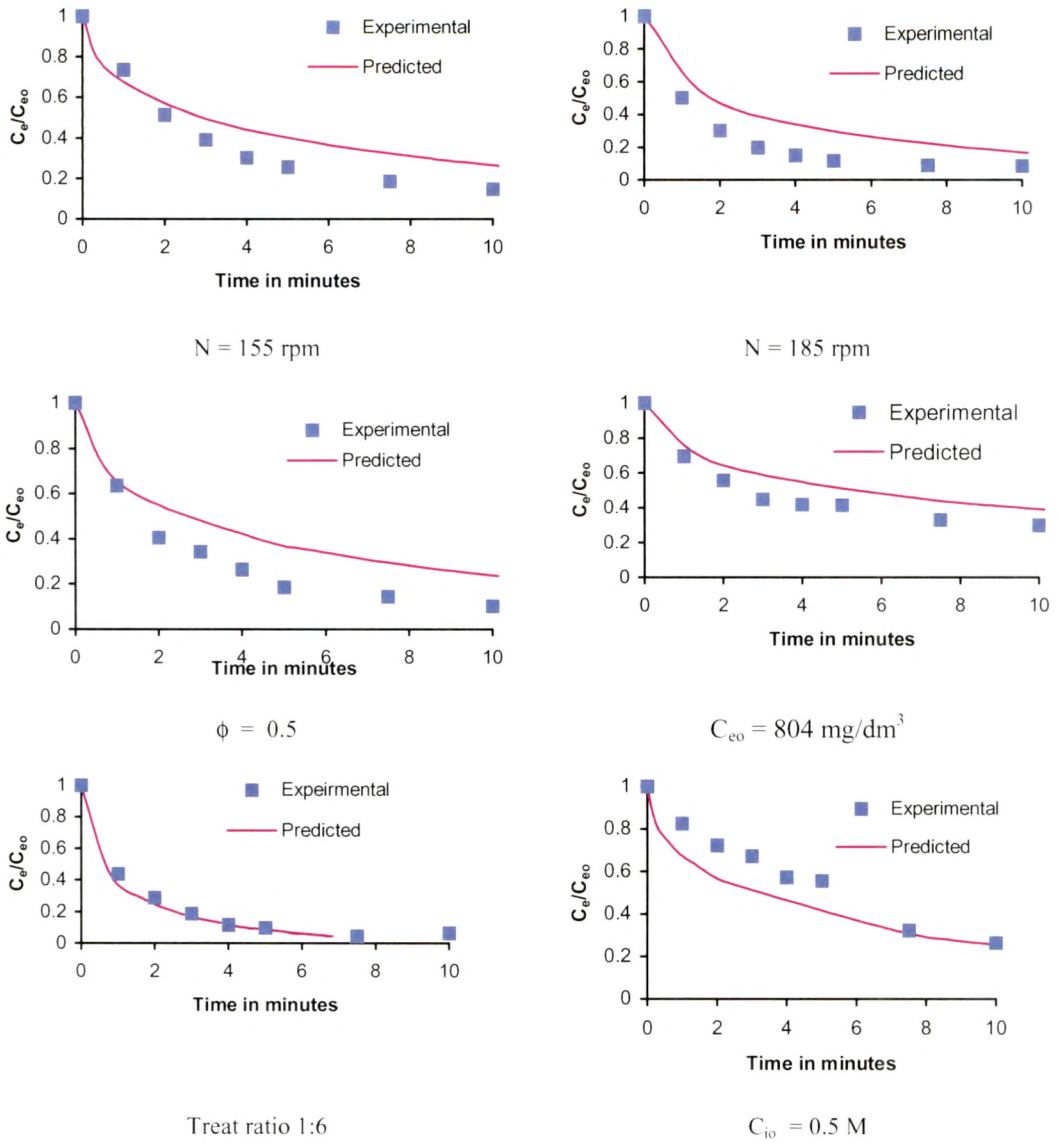

Fig. 6.5: Comparison of experimental and predicted values using AFM (phenol)

6.2 THE REVERSIBLE REACTION MODEL

Bunge and Noble (1984) developed the reversible reaction model in which the reaction between the solute and the internal phase is a reversible one. This model was formulated to address the deficiencies of the advancing front model. The advancing front model tends to

overpredict the removal rate of solute since that approach requires the reagent concentration in the reacted zone between the globule surface and the reaction front to be zero. When the internal reagent is a base such as sodium hydroxide, this requirement is not physically correct. Further, advancing front model assume that the local solute concentration does not affect the amount of reagent to react and that the reagent permanently traps reacted solute. Thus the advancing front models incorrectly predict that even low solute concentrations can force reagent at the reaction front to react completely. Such limitations arise due to the fundamental assumption in advancing front model that the reaction is irreversible.

Bunge and Noble (1984) considered that the reaction between the solute A and internal reagent B is a reversible one and is shown as follows:

$$PhOH + NaOH \rightleftharpoons PhONa + H_2O \qquad 6.24$$

For a general case a solute A diffuses through the globule reacting with reagent a to produce product P solute A distributes through all three phases while reagent B and product P are insoluble in the membrane phase. An equilibrium constant, **K,** characterizes the reversible reaction

$$A + B \rightleftharpoons P \qquad 6.25$$

The assumptions made in this model are the following:

i. The membrane and the external phases are completely immiscible , and the membrane and internal phases are also completely immiscible.
ii. All emulsion globules and internal phase droplets are spherical, and the size of both globules and droplets are represented by a single Sauter men diameter for globules and a single Sauter mean diameter for droplets.
iii. There is no internal circulation within the globules.
iv. Diffusion within the membrane is slow relative to the rate of chemical reaction. Hence, local reaction equilibrium applies through out the globule.
v. Concentration within the internal droplets is independent of position.
vi. Local phase equilibrium holds between the membrane and internal droplet phase. The solute concentration within the globules can be described in terms of the average local concentration.
vii. The system is well agitated so external phase mass transfer resistance can be neglected
viii. Membrane leakage is neglected.
ix. There is no coalescence and redispersion of the emulsion globules

Because B and P are insoluble in the membrane phase, reaction equilibrium applies only in the internal droplets. Neglecting activity effects the equilibrium constant **K** for the reaction (6.25) is

$$\mathbf{K} = \frac{C_{Pi}}{C_{Ai} + C_{Bi}} \qquad 6.26$$

From reagent conservation and reaction stoichiometry, one can derive

$$C^{o}_{Bi} = C_{Bi} + C_{Pi} \qquad 6.27$$

Where C^{o}_{Bi} is the initial concentration of B in the internal droplet phase. Hence C_{Pi} can be obtained by combining Eqs. (6.26) and (6.27).

$$C_{Pi} = \frac{KC_{Ai}C^{o}_{Bi}}{1 + KC_{Ai}} \qquad 6.28$$

Based on assumptions (4) and (6) the membrane phase concentration C_{Am} at any given radial position within the globule can be related to the internal phase concentration of solute A at the same position by the following equation:

$$C_{Ai} = C_{Am} / \alpha \qquad 6.29$$

where α is the distribution coefficient of the solute between membrane and the internal phases. Hence radial variation of C_{Am} induces induces a corresponding position dependence on the internal phase concentrations of A,B and P.

The model equations representing solute concentration in the membrane portion of the globule, C_{Am}, and in the bulk phase, C_{Ab}, as presented by Bunge and Noble (1984) are :

Globule:

$$\frac{\partial C_{Am}}{\partial t} = \frac{D_{eff}}{r^2}\ \frac{\partial}{\partial r}\left(\frac{r^2 \partial C_{Am}}{\partial r}\right) - \left(\frac{1 - f_m}{f_m}\right)\left(\frac{\partial C_{Ai}}{\partial t} + \frac{\partial C_{Pi}}{\partial t}\right) \qquad 6.30$$

$$t = 0 \qquad C_{Am} = 0 \qquad (R > r \geq 0) \qquad 6.31$$

$$r = R \qquad C_{Am} = K_{bm}\, C_{Ab} \qquad (t \geq 0) \qquad 6.32$$

$$r = 0 \qquad \frac{\partial C_{Am}}{\partial r} = 0 \qquad \text{(for all t)} \qquad 6.33$$

Bulk phase

$$\frac{dC_{Ab}}{dt} = \frac{-3D_{eff}(1-f_b)f_m}{Rf_b}\left(\frac{\partial C_{Am}}{\partial r}\right)_{r=R} \qquad 6.35$$

where R is thr globule radius, f_m is the volume fraction of the globule occupied by the membrane phase, f_b is the bulk phase fraction of the total volume, K_{bm} is the partition coefficient between bulk and membrane phase. D_{eff} is the effective diffusivity.

The time derivatives on the right hand side of Eq. (6.30) account for changes in the membrane phase concentration of A by transfer into the internal droplet phase. The transferred solute appears in the internal phase in its reacted and unreacted forms, therefore changes in both C_{Ai} and C_{Pi} must be considered. The second term on the right-hand side of Eq.(6.30) can be conveniently related to the membrane concentration of A by considering phase and reaction equilibria are established between the internal phase droplets and the membrane phase.

$$\frac{\partial C_{Ai}}{\partial t} + \frac{\partial C_{Pi}}{\partial t} = \frac{1}{K_m}\left[1 + \frac{KC^0_{Bi}}{(1+KC_{Am}/K_{im})^2}\right]\frac{\partial C_{Am}}{\partial t} \qquad 6.36$$

Substituting Eq.(6.36) in Eq.(6.30) yields a differential equation in terms of membrane phase concentration only. The equations were rendered dimensionless by Bunge and Noble (1984) by defining the following:

$$\eta = r/R; \qquad \tau = D_{eff}\,t/R^2; \qquad \phi_b = C_{Ab}/C^o_{Ab}; \qquad \phi_m = C_{Am}/C^o_{Ab}K_{bm} \qquad 6.37$$

Further these investigators also defined four dimensionless groups

$$\sigma_1 = f_m[(1-f_b)/f_b]K_{bm} \qquad 6.38$$

$$\sigma_2 = (1-f_m)[(1-f_b)/f_b]K_{bm}/K_{im} \qquad 6.39$$

$$\sigma_3 = K C^o_{Ab} \qquad 6.40$$

$$\sigma_4 = K K_{bm} C^o_{Ab}/K_{im} \qquad 6.41$$

The physical significance of the dimensionless groups are as follows: σ_1 measures the membrane capacity of the solute relative to the bulk phase capacity, σ_2 represents the internal phase capacity for unreacted solute relative to the bulk phase capacity, the original internal reagent and bulk phase solute concentrations are specified as σ_3 and σ_4.

Substituting Eq.(6.37) to Eq.(6.41) in the model equations result in the following model equations:

For globules:

$$\frac{\partial \phi_m}{\partial \tau} = \frac{1}{\eta^2}\frac{\partial}{\partial \eta}(\eta^2 \frac{\partial \phi_m}{\partial \eta})[\frac{1}{1+(\sigma_2/\sigma_1)\{1+\sigma_3/(1+\sigma_4\phi_m)^2\}}] \qquad 6.42$$

$\tau = 0 \qquad \phi_m = 0 \qquad (1 > \eta \geq 0)$ 6.43

$\eta = 1 \qquad \phi_m = \phi_b \qquad (\tau \geq 0)$ 6.44

$\eta = 0 \qquad \partial\phi_m/\partial\eta = 0 \qquad (\text{all } \tau)$ 6.45

For bulk phase:

$$\frac{d\phi_b}{d\tau} = \frac{-3\sigma_1}{f_m}(\frac{\partial \phi_m}{\partial \eta})_{\eta=1} \qquad 6.47$$

$\tau = 0 \qquad \phi_b = 1$ 6.48

The equation (6.42) is highly nonlinear and does not have an analytical solution. The solution of governing equation Eq.(6.42) and Eq.(6.47) was obtained numerically by finite difference explicit schemes on MATLAB® platform. The first derivative terms in the spatial as well as time directions were approximated using a forward difference formulation while the second derivative in spatial direction using the central difference formulation. Explicit scheme is stable if $\alpha \leq 0.5$ where $\alpha = h / k^2$ where h and k are the step size in time and space respectively. As per this restriction the time and spatial step sizes were selected.

6.2.1 Prediction of extraction profiles using the Bunge and Noble model

Numerical solution of the model equations provided a good opportunity to visualize the dynamics of the extraction behavior. Some selected results are presented herewith; the relevant details of the selected runs are presented below:

Parameters	Phenol			o-Cresol	p-Cresol
	Variations			230 mg/dm^3	201.6 mg/dm^3
	TR = 1:6	C_{io} = 0.15 M	C_{eo} = 303 mg/dm^3		
	Case 1	Case 2	Case 3	Case 4	Case 5
C^o_{Ab}(mol/dm^3)	5.36E-03	5.47E-03	3.23E-03	2.13E-03	1.87E-03
C^o_{Bi} (mol/dm^3)	0.3	0.15	0.3	0.3	0.3
f_m	0.55	0.55	0.55	0.55	0.55
f_b	0.8751	0.9375	0.9375	0.9375	0.9375
$K_{im} = K_{bm}$	0.1679	0.1679	0.1679	1.4345	0.8189
K x 10^{-4}(dm^3/eq)	1.1	1.1	1.1	0.63	0.67
σ_1	0.0152	0.0061	0.0061	0.0297	0.0522
σ_2	0.0127	0.0051	0.0051	0.0248	0.0435
σ_3	3300	1650	3300	2010	1890
σ_4	59.18	60.14	35.5	14.27	11.71
A	-0.0836	-0.0335	-0.335	-0.2	-0.2868

The basis of selection was to test the model under variety of conditions where the advancing front model could not give satisfactory results. For example the treat ratio variations were poorly predicted by the advancing front model hence a Treat ratio variation is incorporated, the advancing front model did not predict satisfactorily the results of low feed concentration runs for any system, hence three such runs were incorporated one each for phenol, o-cresol and p-cresol. Further the advancing front model could not predict satisfactorily for low concentration of the reagent phase, hence one run for low internal phase concentration was also incorporated.

The results of these simulations are presented in Fig.6.6 to 6.10. The results are presented as 3 – dimensional visualization of the concentration of solute inside the globule using dimensionless time, dimensionless concentration and dimensionless radius.

♦ Case 1, Fig. 6.6 shows the changing concentration profiles in the surface as well as depth when TR = 1:6 for phenol extraction. It is seen that the surface saturation is about 50 % that changes with time. The penetration of the solute within the globule is very little hence large volume fraction of the globule is free of solute. Although the trend is well depicted in Fig. 6.6 but there is lack of fit with experimental data that shows much greater solute removal.

♦ For Case 2 when C_{io} = 0.15M, the solute (phenol) has to penetrate deep inside the globules in order to get trapped. Such behavior is well depicted in Fig. 6.7 where it is observed that solute penetration is quite deep and the surface layer is almost saturated with the solute. But half the radius is still free of solute.

♦ Case 3 when C_{eo} is 303 mg/dm^3 of phenol it is seen from Fig. 6.8 that the surface layer is almost 70 % saturated and the adjacent surface layers are partially saturated. But again we find that a large fraction of the volume is free of the solute.

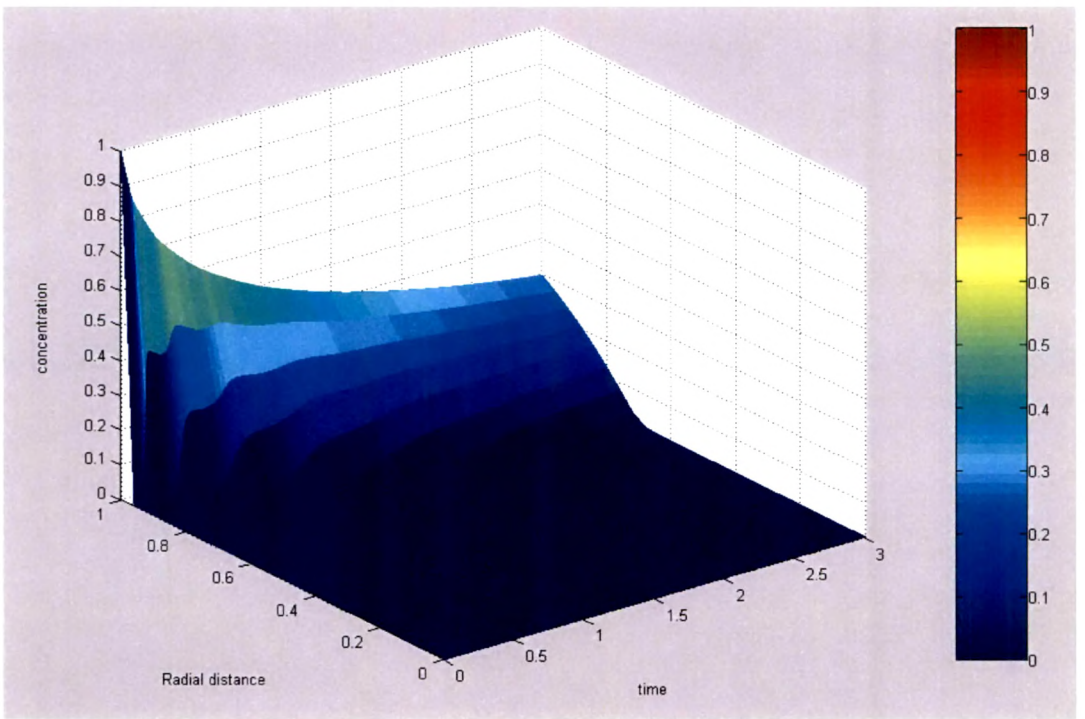

Fig. 6.6:Concentration profile within the ELM globule : Case 1

♦ Case 4 represents o-cresol extraction when the feed concentration is 230 mg/dm^3. Fig. 6.9(a) shows that there is no surface saturation existing, the solute concentration is completely depleted at the surface itself and solute penetration within the globule is minimal. Fig. 6.9(b) shows the comparison of the experimental with predicted values for this case. It is observed that solute removal in the initial stage of experiment is less than the experimentally observed values. However, in the later stages the fit is reasonably good.

♦ Case 5 represents p-cresol extraction when the feed concentration is 201.6 mg/dm^3. Fig. 6.10(a) shows identical behavior as Fig. 6.9 (a) but shows an even better fit when experimental values are compared with the predicted values as shown in Fig. 6.10 (b).

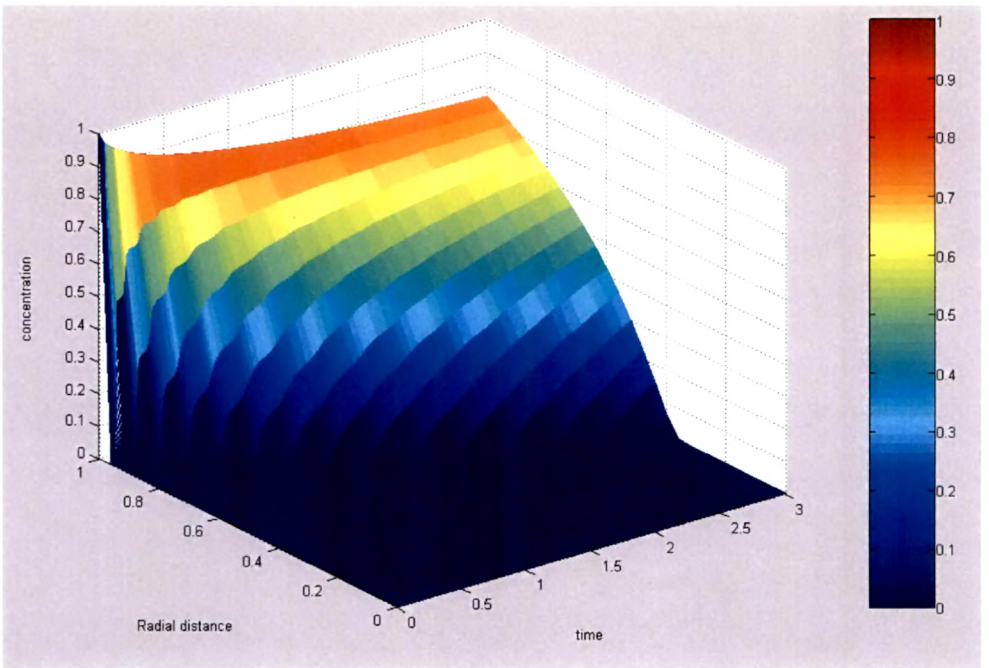

Fig. 6.7: Concentration profile within the ELM globule : Case 2

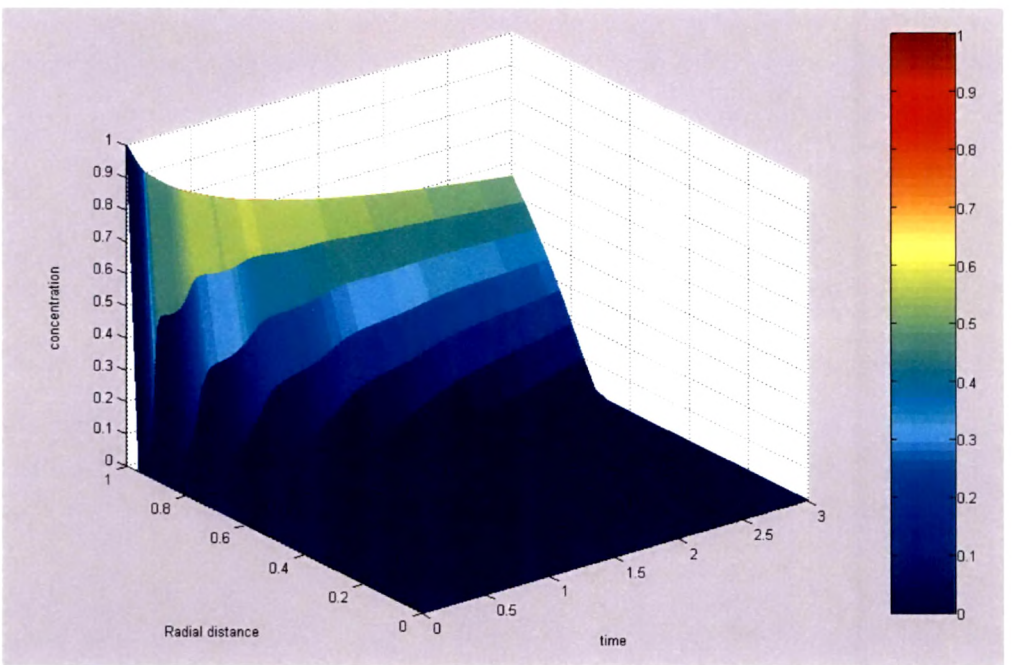

Fig. 6.8: Concentration profile within the ELM globule : Case 3

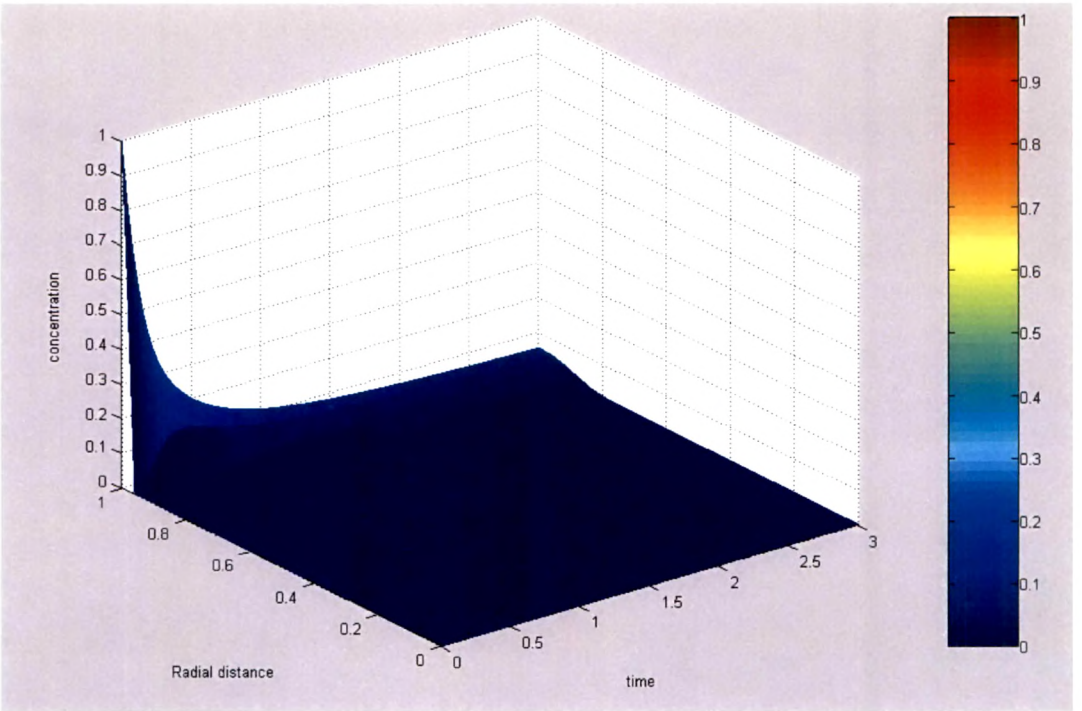

Fig: 6.9 (a)

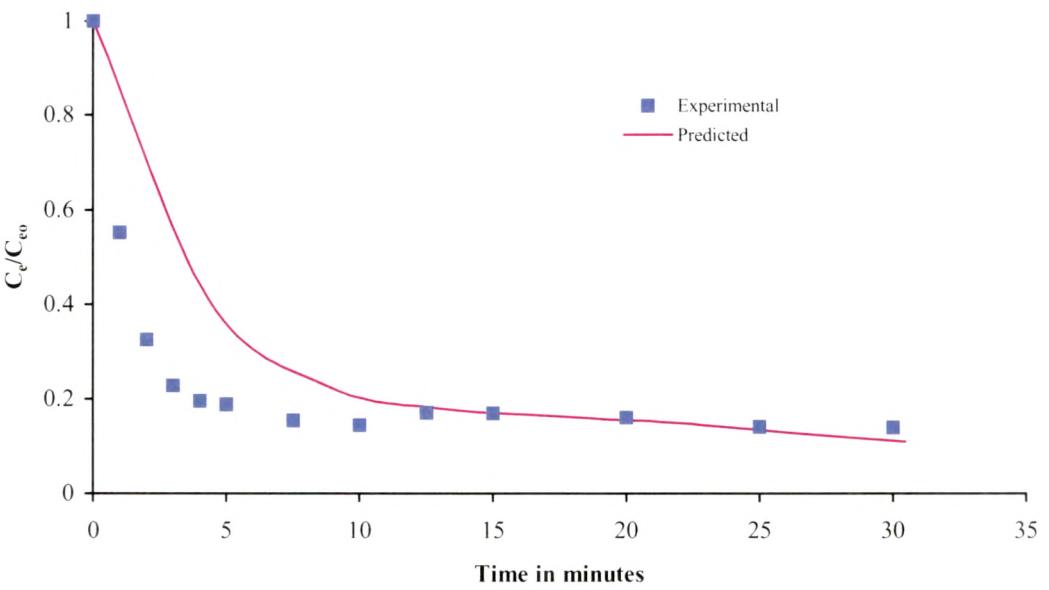

Fig. 6.9 (b)

Fig. 6.9: Concentration profile within the ELM globule : Case 4

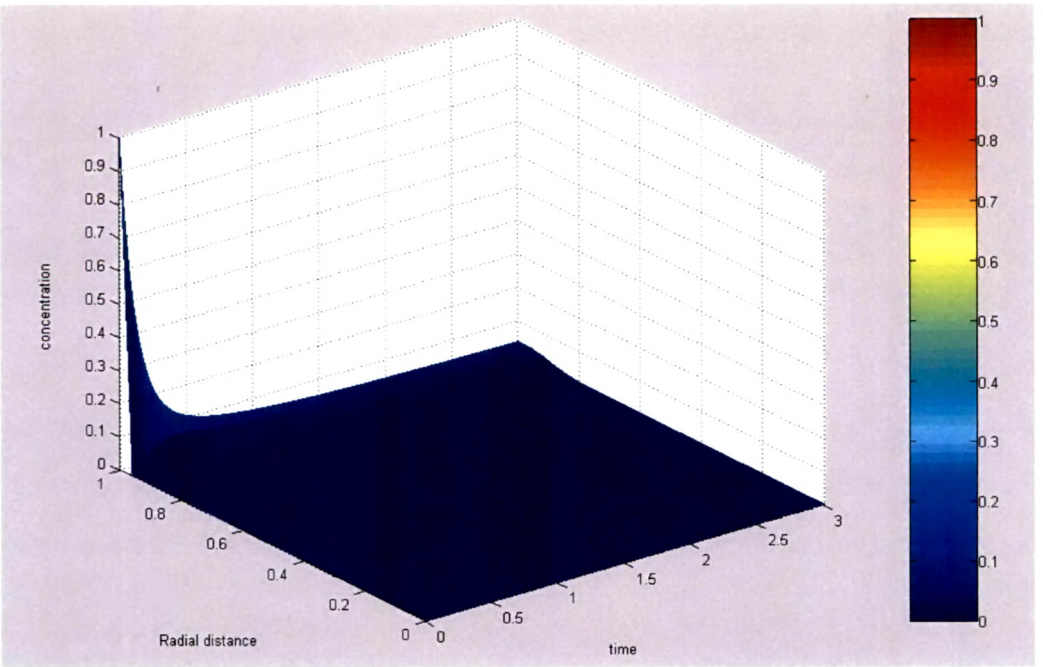

Fig. 6.10 (a)

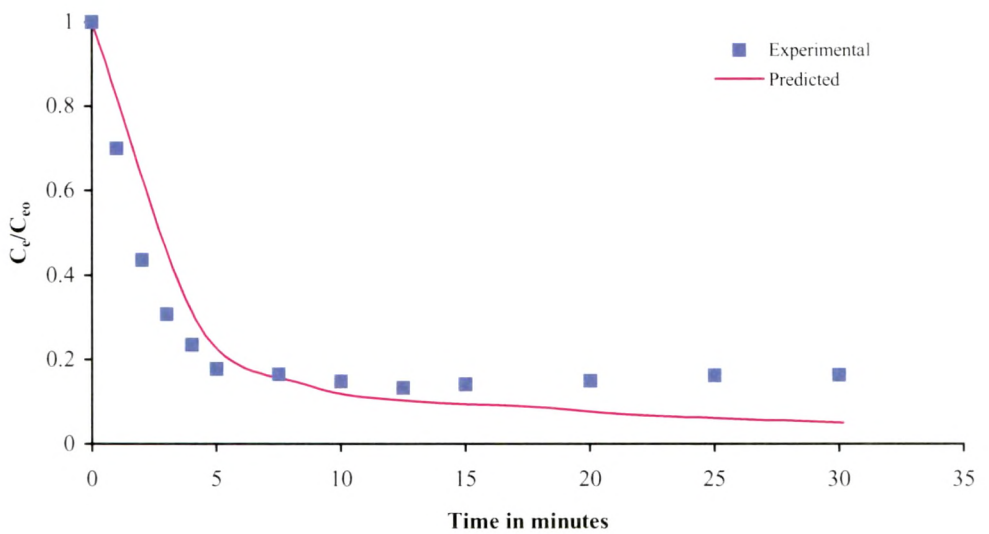

Fig. 6.10(b)

Fig. 6.10: Concentration profile within the ELM globule : Case 5

Thus it is observed that the reversible reaction model predicts well in low concentration ranges where the advancing front model fails due to its inherent assumption of reaction irreversibility.

6.3 SUMMARY

It can be concluded that the emulsion globule approach is a strong mean for understanding the transport mechanism of solutes in to ELMs. This approach does not require to incorporate the mass transfer coefficients in the batch extraction of solutes, which in any case is difficult to determine, and is susceptible to change with process conditions necessitating development of mass transfer correlations.

Two key models of the emulsion globule approach are the advancing front model by Ho *et al.* (1982) and the reversible reaction model of Bunge and Noble (1984). The efficacy of both these models was tested against experimental data for extraction of phenols generated in this study. The advancing front model predicts data very well but at a high feed concentration level, higher the concentration better the results, while the reversible reaction model predicts data reasonably well at lower concentration levels where the advancing front model fails to give appropriate results. Effect of polydispersity of the emulsion globules was noticed and it was felt that in some cases d_{32} is not a very good parameter for quantifying globule diameters.

The key to the successful application of any model rests in the estimation of model parameters such as distribution coefficients, effective diffusivity and the emulsion globule size in the case of advancing front model also the reversible reaction model where an additional parameter of equilibrium constant appears. Although some investigators have used the advancing front model for carrier mediated transport, but due to lack of appropriate data to account for effective diffusivity and equilibrium distribution coefficient for commercial extractants, efforts to predict the solute extraction profiles were not very successful.